15TH IEA HEAT PUMP CONFERENCE
MAY 26–29, 2026 | HOFBURG
VIENNA 2026
DECARBONISATION THROUGH INNOVATION

Predicting Service Life of Heat Pump Refrigerant Cycles Based on Corrosion- and Fatigue-Induced Degradation

L. Mozer[a], M. Drews[a], T. Oltersdorf[a], K.-A. Weiß[a], M. Kolouch[b], L. Schnabel[a*]

[a]Fraunhofer ISE, Heating and Cooling Technologies, Freiburg im Breisgau, Germany
[b]Fraunhofer Institute for Machine Tools and Forming Technologies, Process Technology, Chemnitz, Germany

Abstract

This study develops a specific degradation model for the refrigerant cycle in heat pumps. The model allows a failure time prediction of the refrigerant cycle with respect to the degradation processes corrosion and fatigue. To enhance the model's accuracy, specific stressors (mechanical stress amplitude, mechanical stress cycles, relative humidity and temperature) associated with these degradation processes are derived from measurements and simulations and used to estimate the service life. In the modeling approach, the impact of a defect growing on the surface of a pipe onto the lifetime of the refrigerant cycle is investigated. A literature model was adapted, such that the equation describing corrosion incorporates temperature and humidity. Additionally, an approach to describe the crack growth influenced by both, corrosion and fatigue, is introduced. The study utilizes the simulation result of the mechanical stresses induced by compressor operation at three different frequencies (i.e. 30 Hz, 60 Hz, and 90 Hz), as well as the calculated results of mechanical stresses resulting from thermal expansion. To each frequency belongs a specific location in the refrigerant cycle with maximum mechanical stresses. At each location of maximum mechanical stresses, its unique stressors are determined. Both, mean and maximum values of the stressors are determined to predict the worst-case and mean failure times at the specific location. The results show that at the location of maximum mechanical stresses due to compressor operation at 90 Hz, the failure time calculated using mean stressor values is 19 years; while using maximum stressor values, it is approximately 12 years. For the location of maximum mechanical stresses caused by thermal expansion, the failure time calculated with maximum stressor values is 17 years. The simulation results are integrated into a more comprehensive analysis from simulation and experimental aging of six heat pumps over more than 2 years in the HP Resilience project.

Selection and/or peer-review under the responsibility of the organizers of the 15th IEA Heat Pump Conference 2026.

Keywords: heat pumps; refrigerant cycle; corrosion; fatigue; pit growth; crack growth; Arrhenius–Peck; Paris law; Miner's rule; micro-climate; thermal expansion; compressor vibration; service life prediction; copper (Cu-DHP); accelerated aging

1. Introduction

The global climate is undergoing significant changes, characterized by a rapid increase in the global average temperature [1]. It is accepted in the scientific community that the primary driver of these changes since the mid-20th century is human activity [2]. The concentration of greenhouse gases in the atmosphere, a major contributor to global warming, has risen markedly since the onset of industrialization [3]. In response to climate change, the Paris Agreement [4] was established with the objective of limiting the increase in global mean temperature to below 2°C relative to pre-industrial levels [5].

In 2022, German private households used about 67% of their total end energy consumption for heating and 15% for hot water [6]. Additionally, heating systems that rely on fossil fuels are installed in about 70% of residential buildings in Germany as of 2023 [7]. This data indicates a high potential for reducing greenhouse

* Corresponding author. Tel. +49 761 4588-5907
E-mail address: mathias.drews@ise.fraunhofer.de

gas emissions in the heating of residential buildings. A study analysing various scenarios for achieving a German energy system with a considerable proportion of renewable energy indicates that heat pumps must play a significant role in the decarbonization of the heating sector [8][9]. Heat pumps have a thermal energy output that is several times higher than the electric energy input, because they can extract heat from external energy sources [10].

In practice, installed systems frequently display faults and efficiency shortfalls relative to laboratory conditions [11]. Refrigerant leakage due to a crack in the refrigerant cycle is both common and becomes increasingly safety relevant as the use of natural refrigerants, which are flammable, expands [12]. Failure analyses of copper tubing in refrigeration systems consistently identify corrosion and fatigue as the dominant degradation mechanisms behind leakage [13].

To support the industry in extending the service life of refrigerant cycles, a crack-growth model has been developed. This model enables the simulation of crack initiation and propagation on the surface of copper tubing used in refrigerant circuits, accounting for both, atmospheric corrosion and fatigue, which are both influenced by its operational stressors. The evolution of surface defects is represented in two stages: an initial phase of corrosion-driven pit growth up to a crack-initiation threshold, followed by fatigue-driven crack propagation, during which corrosion continues to contribute to crack deepening. To enhance the accuracy of the simulation, stressor values influencing pit and crack growth were quantified and incorporated into the model.

2. Methods/Approach

Modelling the degradation of refrigerant cycles in heat pumps requires a framework that captures the combined effects of corrosion and fatigue under realistic operating and environmental conditions. Unlike many idealized laboratory models, heat pumps experience complex and varying loads that must be reflected in the modelling approach. Two degradation mechanisms are particularly relevant: atmospheric corrosion, which depends strongly on climatic conditions, and mechanical fatigue, which results from the operation of the heat pump. Therefore, first the characteristics of the use case are presented. In the second chapter, the adaption of the literature model is presented.

Characteristics of the Use-Case

In real systems, the two degradation modes, corrosion and fatigue, interact and often reinforce one another, meaning that materials degrade faster when exposed to both corrosion and mechanical stress cycling than when subjected to only one of these influences. A suitable model must therefore represent this synergistic behaviour rather than treating each mechanism independently.

A key characteristic of the use case is that fatigue does not occur continuously. Mechanical fatigue is primarily driven by compressor operation, which induces vibrations, pressure fluctuations, and thermal expansion cycles in the piping system. These loads only occur when the compressor is running. Corrosion, on the other hand, can occur at any time, provided that temperature, humidity, and chemical pollutants promote the formation of a corrosive environment on the pipe surface. As a result, corrosion progresses continuously whenever conditions permit, while fatigue progresses intermittently. Any realistic modelling approach must therefore separate these two timescales and combine them appropriately.

Another challenge arises from the variability of mechanical loads. In practical installations, heat pumps operate at different compressor frequencies, experience temperature-driven expansion and contraction, and undergo start-up and shutdown oscillations. Each of these effects results in different stress amplitudes and different numbers of load cycles. A flexible degradation model must therefore be able to incorporate multiple stress amplitudes and load types rather than relying on a single constant stress level.

Environmental conditions represent another important complexity. Heat pumps can be installed in a wide range of climates with varying temperature and humidity profiles. Local weather patterns, seasonal variations, and even the operation of the heat pump itself influence surface conditions on the refrigerant pipes. When the heat pump is running, parts of the refrigerant cycle heat up while others cool down, directly influencing the local surface humidity. Additionally, pollutants such as chloride or sulphur dioxide may be present depending on the installation site, for example near industrial areas, traffic, or biomass combustion. Since corrosion is highly sensitive to these environmental factors, the degradation model must incorporate time-dependent climatic conditions and be able to predict degradation for site-specific microclimates.

To summarize, a modelling framework capable of representing the degradation of the refrigerant cycle must fulfil the following requirements:

- Synergetic behaviour of corrosion and fatigue must be included.
- The timescales for both degradation modes must be separated.
- The modelling approach must incorporate different stress amplitudes.
- It must be possible to describe the corrosion kinetics dependent on the environmental influences.

The Modelling Approach

The combined corrosion–fatigue modelling approach is based on a literature model [14] that divide crack formation and growth into three phases: pit formation, surface crack growth, and through-wall crack growth. For predicting failure, only the first two phases are relevant, since leakage occurs once a through-wall crack forms. Figure 1, illustrates the defect growth and its phases. It shows that corrosion influences both phases, whereas fatigue only leads to crack growth in the second phase. Also, the transition from the first to the second phase is shown. In this work, the chosen stressors for corrosion are temperature and relative humidity, while for fatigue it's the stress amplitudes and the number of stress cycles, which depends on the operation time of the compressor.

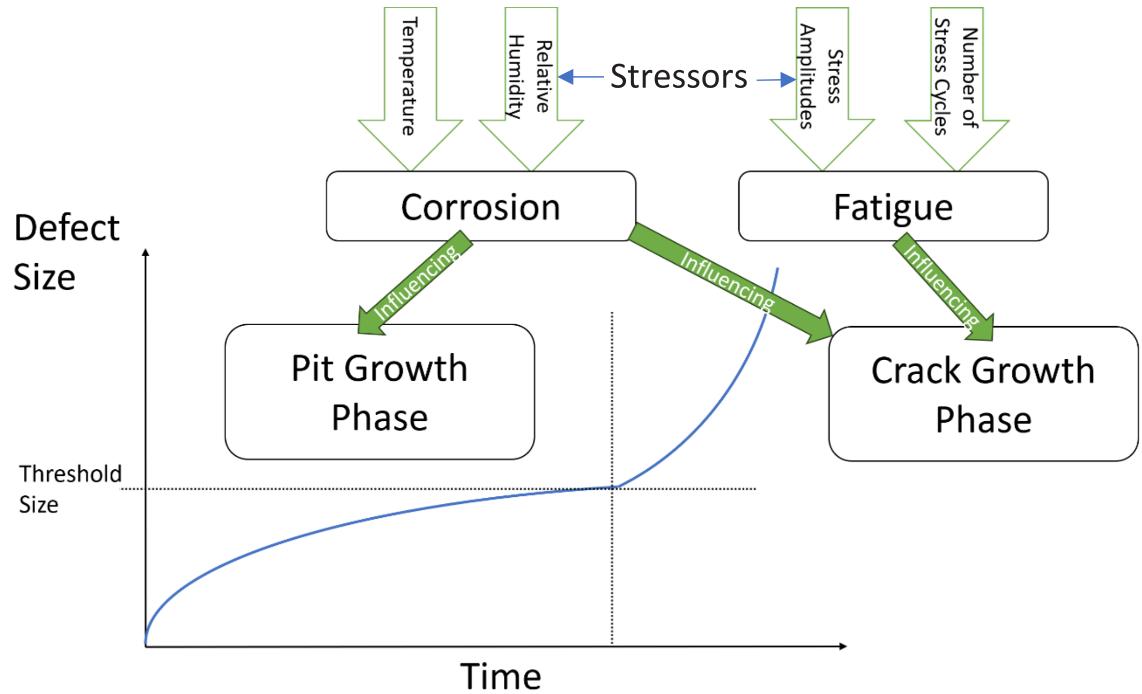

Figure 1: Schematic illustration of the Modelling approach.

The simulation approach is based on evaluating crack growth in discrete time intervals to incorporate the varying stressors associated with the different degradation mechanisms. In this work, a monthly interval is selected. To account for the distinct timescales of corrosion and fatigue, the contributions of each mechanism to crack growth are computed separately within each interval and subsequently summed. The resulting defect size then serves as the initial condition for the subsequent interval, ensuring that the evolving geometry consistently influences the progression of damage over time.

In the first phase, degradation is dominated by corrosion, a pit growing on the pipe surface is modelled using the Faraday Law and an accelerated aging formulation. An environmental acceleration factor $\boldsymbol{AF_i}$ of the time interval $\boldsymbol{i}$ accounts for how temperature $\boldsymbol{T}$ and humidity $\boldsymbol{RH}$ increase the corrosion rate in the observed time interval. This allows pit depth $\boldsymbol{a_i}$ to be computed as a function of time under varying atmospheric conditions. Since the pit depth $\boldsymbol{a_i}$ at the end of the time interval must be determined and the intervals can have different atmospheric conditions, a reference time

$$\boldsymbol{t_{i,ref} = AF_i \frac{2\pi n F\rho}{3MI_P} a_{i-1}^3},$$

for each time interval must be determined, where $\boldsymbol{n}$ is the valence number, $\boldsymbol{F}$ Farday´s constant, $\boldsymbol{\rho}$ the density of the material, $\boldsymbol{M}$ the relative atomic mass, $\boldsymbol{I_P}$ the corrosion current and $\boldsymbol{a_{i-1}}$ the pit depth at the end of the last time interval. $\boldsymbol{t_{i,ref}}$ can be interpreted as the time, the pit would need to grow to the pit size at the beginning of the interval at the atmospheric conditions of the time interval. This ensures a continuous growth of the pit. To calculate the pit size $\boldsymbol{a_i}$ the following equation can be used

$$\mathrm{a_i} = \left(\frac{3\mathrm{M}\boldsymbol{I_P}(\boldsymbol{t_{i,ref}} + \Delta \boldsymbol{t})}{2\pi \mathrm{nF}(\boldsymbol{AF_i})\boldsymbol{\rho}}\right)^{\frac{1}{3}},$$

with Δt as the time of a time interval.

The acceleration factor can be defined by an accelerated aging model, in this work the Arrhenius-Peck model was used, as it incorporates both stressors on which corrosion in this work should depend [15]. It is defined by

$$AF_i(T, RH) = A\left(\frac{RH}{RH_0}\right)^B exp\left[-\frac{E_a}{k_B}\left(\frac{1}{T} - \frac{1}{T_0}\right)\right],$$

Where RH_0 is the reference relative humidity, T_0 is the reference temperature, A, B are model constants, E_a is the activation energy and k_B is the Boltzmann constant.

Transition from pit formation to crack initiation occurs when the pit reaches a threshold depth at which the stress intensity factor $\Delta\boldsymbol{K}(\boldsymbol{S_a}, \boldsymbol{a})$ equals the threshold stress intensity factor $\Delta\boldsymbol{K_{th}}$ for the material, which can be determined by

$$\Delta\boldsymbol{K}(\boldsymbol{S_a}, \boldsymbol{a}) \geq \Delta\boldsymbol{K_{th}}.$$

In the second phase, both corrosion and fatigue contribute to crack growth. In the modelling approach presented here, the two mechanisms are treated independently within each time interval and combined at the end of that interval. Fatigue-driven crack growth is computed using established crack-growth equations based on the stress amplitude distribution and the stress intensity factor. The adapted equation is given by

$$N = \int_{a_{i-1}}^{a_{i,Stress}} \int_{S_{a,min}}^{S_{a,max}} \frac{1}{C\big(\Delta K(S_a, a)\big)^m} f(S_a) d\, S_a da,$$

Where C, m are model parameters, $S_{a,max}$ and $S_{a,min}$ are the maximal and minimal occurring stress amplitude, $a_{i,Stress}$ is the crack size grown by fatigue in the time interval and $f(S_a)$ is the density distribution of the stress amplitudes in the time interval.

In parallel, corrosion continues to enlarge the pit according to the same corrosion model used in the first phase, again adjusted by an environmental acceleration factor. To calculate it only the pit growth $\Delta\boldsymbol{a_{i,Pit}}$ in the second phase must be calculated by

$$\Delta a_{i,Pit} = a_{i,Pit} - a_{i-1,Pit},$$

Where $a_{i,Pit}$ is the pit size at the end of the time interval i and $a_{i-1,Pit}$ the pit size in the beginning.

The corrosion-induced deepening of the pit and the fatigue-induced crack extension are then summed to determine the total crack depth $\mathbf{a_i}$ at the end of each interval. The equation is given by

$$a_i = a_{i,Stress} + \Delta a_{i,Pit}$$

This process is repeated across successive time intervals with evolving mechanical and environmental loads until the crack reaches a critical size, at which the pipe wall can no longer sustain internal pressure and failure occurs, which is here chosen to be $\mathbf{0.7 \cdot d}$, with $\boldsymbol{d}$ the thickness of the pipe.

3. Results and Discussion

In this section, the micro-climatic loads are first quantified, followed by the determination of the model parameters, and finally the presentation of the simulation results.

Micro climatic loads

This section quantifies the mechanical and environmental stressors at locations in the refrigerant circuit where degradation is expected to occur most rapidly. Since stressor levels—mechanical stress amplitudes, temperature, and relative humidity—vary along the circuit, the analysis focuses solely on points exhibiting the highest mechanical loading. For these critical locations, the corresponding thermal and hygroscopic conditions, including both peak and mean values, are determined to provide the inputs required for subsequent defect-growth and lifetime modelling.

<u>Mechanical stress</u>

Cyclic stresses in the refrigerant circuit originate primarily from compressor-induced vibrations and thermally driven expansion of the copper piping. Pressure-related stress cycles and transient start-up or shut-down oscillations were not considered, as simulations confirmed that their amplitudes and cycle counts are negligible compared to those occurring during steady operation. The vibration-induced stresses depend strongly on the piping geometry and the compressor frequency; therefore, harmonic finite-element analyses were performed at 30 Hz, 60 Hz, and 90 Hz to identify the corresponding maximum stress amplitudes and their locations. Each simulation provided a representative stress–time waveform, including beat patterns caused by modal superposition, which were used to determine both maximum and effective cyclic stress amplitudes. Because the compressor operates in a broader frequency range (15–110 Hz), nonsimulated frequencies were approximated by the nearest simulated case. Monthly stress-cycle counts were estimated by combining annual operating-hour data [16] with monthly heating-demand distributions [17] and by assuming a uniform frequency distribution.

The first analysed frequency is 30 Hz. The stress amplitude peaks at a pipe, that is connected to the inlet of the compressor. The location of the maximum stress amplitude is illustrated in Figure 2. The maximum stress amplitude occurring at this frequency is 4.9 MPa. For the mean value of the cyclic loads a beat must be determined for this frequency. For this frequency there is no beat observable in the simulated stress time curve. Therefore, for the mean value of the cyclic loads of this frequency, it is assumed that the maximum stress amplitude occurs in every cycle. The stress amplitudes oscillate with the compressor frequency.

The second analysed frequency is 60 Hz. The stress amplitude peaks at the pipe, which relates to the outlet of the compressor. In Figure 2, the location of maximum mechanical stresses can be observed. The maximum stress amplitude observable at this spot is 6.3 MPa. For the mean value of the cyclic loads the cycles in a beat have to be determined. There are 3 cycles in a beat for this frequency. Therefore, it is assumed that every 3 cycles a maximum stress amplitude occurs and the other two are stress amplitudes that have the value of half the maximum stress amplitude. The stress amplitudes are oscillating at the according compressor frequency.

The last analysed frequency is 90 Hz. The location of the maximum stress amplitude is again located on the pipe at the inlet of the compressor, but at a different bend as the 30 Hz maximum stress location. In Figure 2, this location of maximum stresses is observable. The maximum observed stress amplitude is 21.3 MPa. In a beat there are 4 cycles. That means for the mean value of the cyclic loads, every fourth cycle is a cycle with the maximum stress amplitude at that location. The frequency of the stress amplitudes is the same as the according compressor frequency.

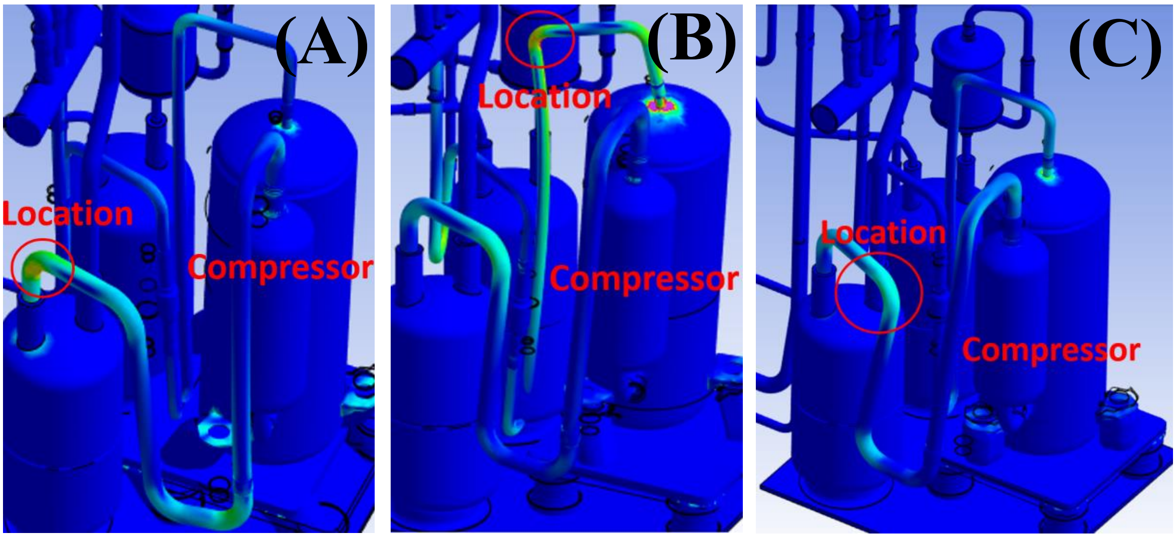

Figure 2: Result of the FEM-Simulation; (A) shows the result for 30 Hz (B) shows the result for 60 Hz, (C) shows the result for 90 Hz.

Thermally induced stresses were evaluated separately at the steel–copper interface of the compressor outlet, where differences in thermal expansion coefficients produce additional cyclic loading. The thermal stress amplitude was calculated using

$$S_a = E(\alpha_{Cu} - \alpha_S)\Delta T,$$

where E is the Young´s Modulus, α_{Cu} and α_S the thermal expansion coefficients of Copper and steel and ΔT the temperature difference. Yielding in mean and maximum amplitudes of 20.5 MPa and 34.1 MPa, respectively. Since thermal cycles occur once per compressor start-stop event, their monthly frequency was derived from monitored annual cycling data and scaled by monthly heating demand.

At every location where a maximum cyclic stress amplitude was identified—whether vibration-induced or thermally induced—a dedicated crack-growth simulation will be performed. These critical points therefore serve as the basis for the subsequent fracture-mechanics analysis and lifetime estimation.

<u>Temperature</u>

The temperatures at the locations of maximum stress were determined separately for the cold and hot sides of the refrigerant cycle. At the two stress maxima located at the compressor inlet (corresponding to 30 Hz and 90 Hz operation), the pipe temperature during compressor operation is approximately 3 K below ambient temperature. The two stress maxima on the hot side—at the compressor outlet during 60 Hz operation and at the steel–copper connection—reach temperatures about 5 K above the heating-flow temperature. Monitoring data from 36 residential heat pumps indicate typical heating-flow temperatures that justify assuming a mean outlet-pipe temperature of 45 °C and a maximum of 75 °C. The pipe wall is assumed to be isothermal with the refrigerant, and its temperature is taken to change instantaneously with compressor on/off states. Ambient conditions are represented by the monthly average temperatures recorded in Germany in 2024 [18].

<u>Relative Humidity</u>

Relative humidity at the critical pipe locations differs from the ambient value because it varies with surface temperature. As the maximum steam density increases with temperature while absolute vapor density remains constant, the relative humidity at the pipe surface during compressor operation must be corrected accordingly. This adjustment is performed using the Magnus equation. During operation, the pipe surface humidity is assumed to instantaneously adopt the temperature-corrected value; once the compressor switches off, it returns to the ambient level. Using monthly average ambient humidity data for Germany [19], the calculations show that relative humidity at the cold compressor inlet approaches 100% during operation, while at the hot outlet it drops to extremely low levels (e.g., 6% at mean outlet temperature and 1.8% at maximum) during operation. These strong humidity gradients play a significant role in the subsequent determination of the acceleration factor.

Calculation of the acceleration factor

To account for the influence of temperature and relative humidity on corrosion, a time-averaged acceleration factor must be determined, since the heat pump alternates between operating and idle states. Corrosion growth is modelled using the Arrhenius–Peck formulation, and the effective acceleration factor over a given interval is obtained as a weighted average of the “on” and “off” conditions.

Model parameters

In the following, the model parameters are derived, beginning with those associated with the corrosion model and subsequently those governing crack growth.

Arrhenius-Peck model

A statistical mass-loss model is employed to estimate corrosion rates under varying climatic conditions, because the specific experimental data needed is not available yet. After determining the critical pit size and the corresponding required mass loss, the time to reach this mass loss is computed for different combinations of temperature and humidity. A calibration factor is introduced to reconcile the Faraday-based and statistical mass-loss formulations. Using the calibrated statistical model, crack-initiation times are generated across a defined range of climatic conditions, from which acceleration factors are calculated. These factors are finally fitted using the Arrhenius–Peck model, yielding the parameters of the accelerated aging model. The parameters can be observed in Table 1. With ongoing work, these parameters must be determined by specific experiments.

Table 1: Arrhenius-Peck model parameters

Parameter	Value	Standard deviation
A	0.021244	0.000114
B	0.19039	0.025233
E_a	0.11591 eV	0.018637 eV

Faraday Model

To apply the Faraday mass-loss model, the corrosion current must first be determined. Based on experimental data for copper at pH ≈ 5.2—representative of German rainwater—the corrosion current density is taken as 9 µA/cm² under 100% relative humidity and an assumed temperature of 18 °C [20]. Since only the current density is known, the effective corrosion area is estimated from the critical pit geometry. Using a critical pit radius of 0.33 mm, the surface area of a half-spherical pit is calculated, with assumptions that corrosion affects 50% of this area for the mean case and 33% for the maximum case. This yields corrosion currents of 0.123 µA (mean) and 0.1845 µA (maximum).

Table 2: Parameters of the Faraday Model.

Parameter	Value	Standard deviation
I_P	0.123 / 0.1845 µA	0.06125 / 0.09225 µA
n	29	-
F	96485.33 C/mol	-
M	63.55 g/mol	-
ρ	8960000 g/m^3	-

In Table 2, the parameters of the Faraday model are displayed. Here it is assumed, that the literature values have no standard deviation.

Crack growth equation

Table 3 summarizes the parameters used in the crack-growth equation [21][22]. Here it is assumed, that these literature parameters do not have an standard deviation.

Table 3: Parameters of the crack growth equation.

Parameter	Value
C	$2.95 \cdot 10^{-12}$
m	3.5
ΔK_{th}	2.5 $\mathrm{MPa}\sqrt{\mathrm{m}}$

Simulation Results

The following section presents the simulation results for each location exhibiting maximum mechanical stress. The heat pump examined in this study employs the copper alloy CU-DHP, a grade characterized by very high purity. The refrigerant pipes in the analysed system have a nominal wall thickness of 1 mm.

Compressor operation at 30 Hz

The Figure 3 shows the evolution of the defect size over time and indicates that, at this location, the critical pit depth required for crack initiation exceeds the defined failure threshold. Consequently, the defect never transitions into a crack before leakage occurs, and pit corrosion alone governs degradation. This outcome is primarily due to the low maximum stress amplitude, which results in a large critical pit size. The results further show that higher stressor values accelerate degradation: the predicted failure time decreases from

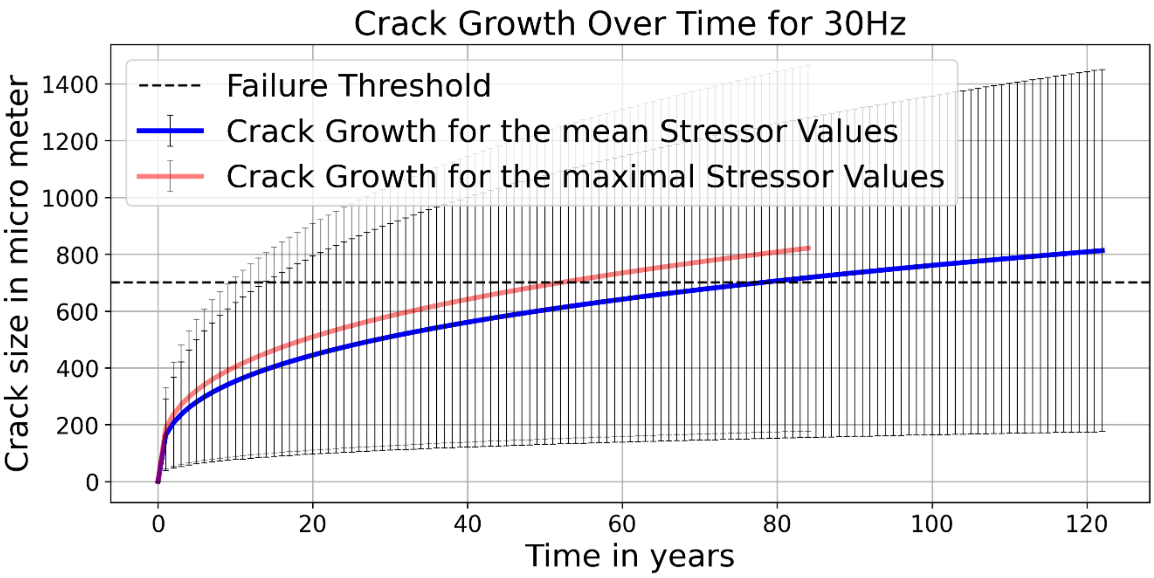

Figure 3:Defect progression at the 30 Hz inlet bend.

approximately 78 years (mean stressor values) to about 52 years (maximum stressor values). Because the failure threshold is author-defined based on the onset of high crack-growth geometry factors, extending the calculation beyond this point shows that pit growth would continue for an additional ~30 years under both stressor scenarios.

Generally, it is possible to say, that at this location of maximum mechanical stresses due to normal compressor operation at 30 Hz, with the considered stressor values it is unlikely, that at this location leakage occurs, during a common lifetime of the heat pump.

Compressor operation at 60 Hz

Figure 4 shows the defect-size evolution for the mean and maximum stressor conditions. As in the previous case, the critical pit depth required for crack initiation lies above the defined failure threshold, meaning that failure occurs within the pit-growth phase and no crack growth is triggered. The large critical pit size again results from the low maximum stress amplitude. Higher stressor values accelerate degradation, reducing the predicted failure time from approximately 77 years (mean values) to about 51 years (maximum values). Even under the maximum stress conditions, the resulting lifetime remains high, and the continued slow pit growth

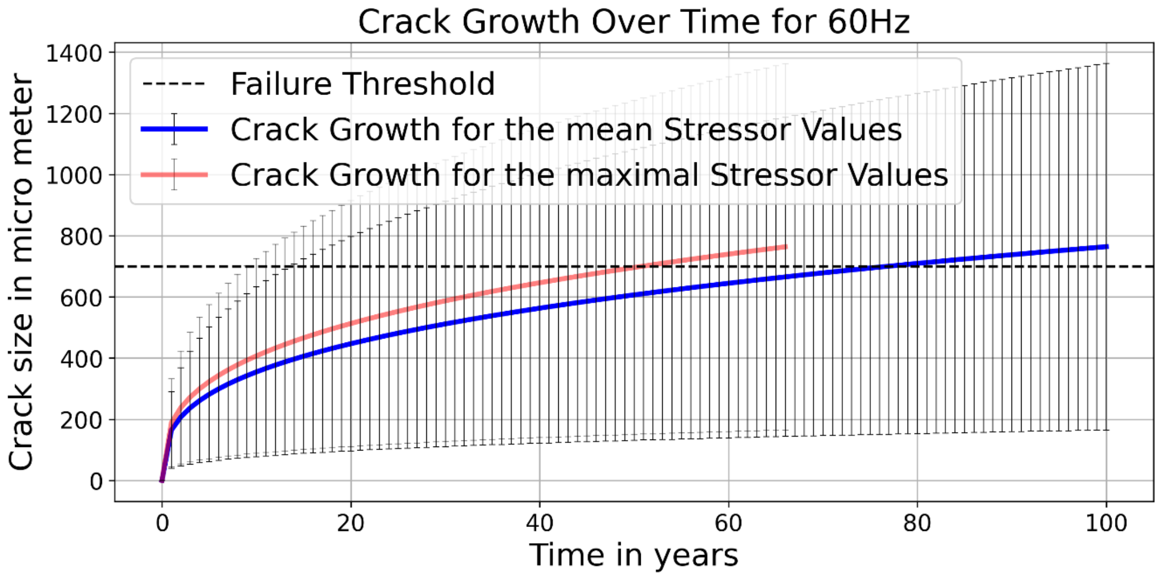

Table 4: Defect progression at the location of maximum mechanical stresses at 60 Hz compressor operation.

beyond the threshold suggests an even longer effective service life. Overall, leakage at this 60 Hz maximum-stress location is unlikely during the typical lifetime of a residential heat pump.

Compressor operation at 90 Hz

Figure 5 presents the defect-size evolution for both mean and maximum stressor conditions. At this 90 Hz maximum-stress location, the stress amplitude is substantially higher than at the 30 Hz and 60 Hz locations, resulting in a much smaller critical pit size of approximately 430 µm. Once this size is reached, the defect

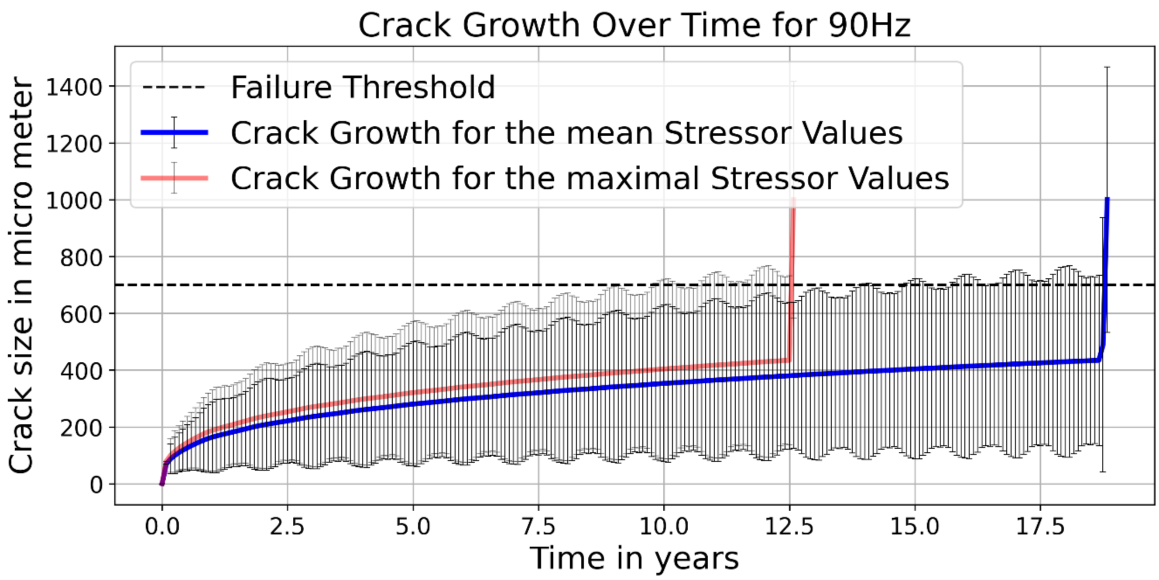

Figure 4: Defect progression at the 90 Hz inlet bend.

rapidly transitions into the crack-growth phase, where crack propagation proceeds quickly due to the high number of load cycles. Consequently, the predicted failure times are significantly shorter: about 12 years under maximum stressor values and roughly 19 years under mean conditions. These results indicate that leakage at this location is likely within the typical service life of the heat pump.

<u>Thermal expansion at the compressor outlet joint</u>

Figure 6 illustrates the defect evolution at the location where thermal expansion induces the highest mechanical stresses. Under maximum stressor conditions, the defect enters the crack-growth phase after only ~3 years, driven by both high corrosion stressors and a high stress amplitude. In contrast, when mean stressor values are applied, the pit-growth phase persists for roughly 20 years before crack initiation occurs, reflecting lower corrosion severity and reduced mechanical loading. The failure threshold is subsequently reached after about 17 years for the maximum-stressor case and approximately 43 years for the mean-stressor case.

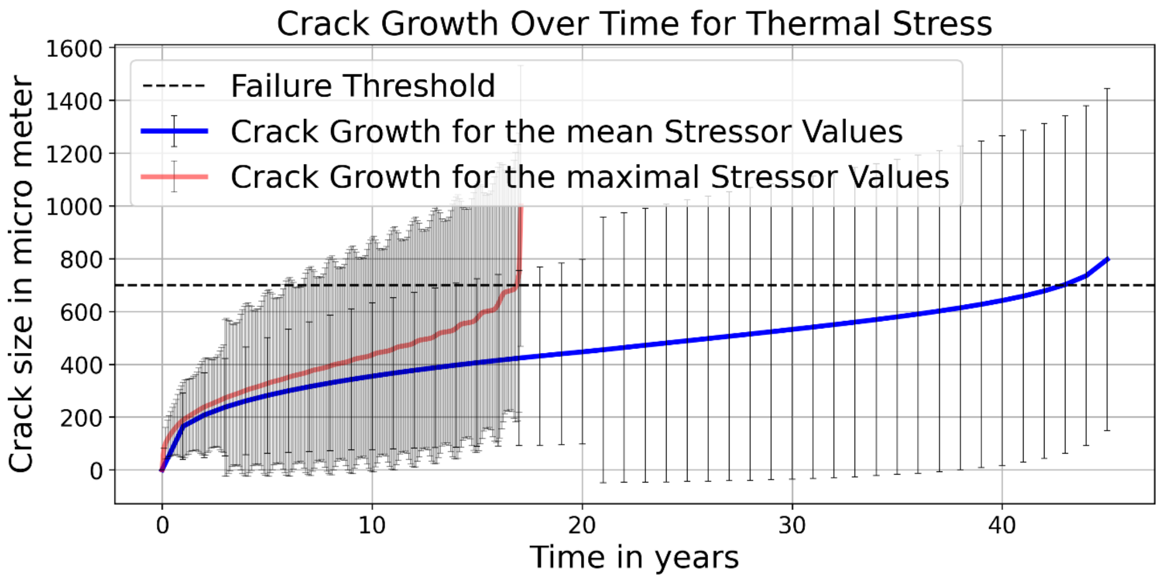

Figure 5: Defect progression at the compressor outlet joint.

Table 4 summarizes the predicted failure times for each location under both mean and maximum stressor conditions.

Table 4: Predicted failure time by location.

Location of maximal stress	Stress source	Stress amplitude(s)	Failure time (mean stressors)	Failure time (max stressors)
30 Hz	Compressor vibration	≈ 4.9 MPa	≈ 78 years	≈ 52 years
60 Hz	Compressor vibration	≈ 6.3 MPa; 3-cycle beat	≈ 77 years	≈ 51 years
90 Hz	Compressor vibration	≈ 21.3 MPa; 4-cycle beat	≈ 19 years	≈ 12 years
Thermal stress	Thermal expansion	≈ 20.5 MPa (mean); ≈ 34.1 MPa (max)	≈ 19 years	≈ 19 years

Discussion

This section evaluates the proposed degradation model for a heat-pump refrigerant cycle and discusses its results at four critical stress locations. The underlying literature model describes defect evolution driven by corrosion and fatigue, assuming hemispherical pit growth. Because real pit geometries may vary, failure times can differ accordingly.

Two major adaptations to the literature model were required. First, an accelerated aging model based on monthly climatic averages was integrated into the pit-growth formulation. This raises the question of whether averaged humidity values sufficiently represent the actual corrosion process, which depends on the intermittent formation of electrolyte films. Second, corrosion was included during crack growth to account for intervals with few mechanical load cycles—an assumption supported by the results at the thermal-expansion stress location. In contrast, at locations with high cycle counts (normal compressor operation), corrosion has negligible influence on crack growth.

Overall, the adjusted model captures the degradation behavior plausibly. Higher stressor values consistently accelerate defect growth, and locations with low mechanical stress amplitudes (30 Hz and 60 Hz) show long lifetimes, while the 90 Hz and thermal-expansion locations degrade significantly faster. One inconsistency arises: the model predicts faster pit growth on the hot side of the refrigerant cycle despite its low operating humidity. This mismatch likely stems from overestimation of temperature effects in the accelerated aging model and could be resolved using dedicated experimental calibration.

The 90 Hz location shows the shortest lifetime (~19 years under mean conditions), which aligns well with expert expectations of air source heat-pump service life (15-20 years) [21][22]. For thermal-expansion stresses, the predicted lifetimes vary widely (17–43 years), driven by large differences between mean and maximum stress amplitudes and cycle counts. Only a small proportion of heat pumps fail at this location. However, for failures within the refrigerant cycle, the position experiencing the highest mechanical stresses during 90 Hz compressor operation is the dominant failure point.

4. Conclusions

A physics-of-failure framework was developed and applied to predict service life of heat pump refrigerant cycles under coupled atmospheric corrosion and cyclic mechanical fatigue. The two-phase approach—corrosion-driven pit growth to crack initiation followed by fatigue-driven crack propagation while corrosion continues interval-wise—captures the dominant mechanisms under realistic stress spectra and micro-climatic loads. Using location-specific stresses from harmonic analysis and thermal expansion, monthly operating shares and cycles, and surface humidity/temperature corrections via the Magnus relation, the model yields plausible service-life estimates: over 50 years at low-stress vibration locations (30/60 Hz), approximately 19 years (mean stressors) and 12 years (max stressors) at a high-stress 90 Hz location, and approximately 43 years (mean stressors) or 17 years (max stressors) at the thermal expansion joint. The outcomes are consistent with expert assessments of typical lifetimes and with known mechanics. Future work should parameterize the corrosion acceleration with targeted pit-depth experiments across T/RH, validate predictions against accelerated tests on instrumented systems, and refine transient surface micro-climate and pit-geometry assumptions. Extending the framework to internal corrosion scenarios is possible with appropriate adaptation of the micro-environment and kinetics.

References

1. Rebecca Lindsey and LuAnn Dahlman. “Climate change: Global temperature”. In: Climate. gov 16 (2020).
2. Mark Richardson, Kevin Cowtan, and Richard J Millar. “Global temperature definition affects achievement of long-term climate goals”. In: Environmental Research Letters 13.5 (2018), p. 054004.
3. Thomas F Stocker. “21 IPCC Working Group I: The Swiss contribution 1988– 2014”.
4. United Nations. The Paris Agreement. https://unfccc.int/sites/default/ files/resource/parisagreement_publication.pdf. Accessed: (01.11.2025). 2016.
5. Tianyu Li et al. “Towards Paris Climate Agreement goals: The essential role of green finance and green technology”. In: Energy Economics 129 (2024), p. 107273.
6. Umwelt Bundesamt. Energieverbrauch privater Haushalte. Accessed: (10.11.2024). 2024. URL: https://www.umweltbundesamt.de/daten/private-haushaltekonsum / wohnen / energieverbrauch - privater - haushalte # hochster - anteil-am-energieverbrauch-zum-heizen.

7. BDEW Bundesverband der Energie-und Wasserwirtschaft e.V. Studie: Wie heizt Deutschland 2023? Accessed: (10.11.2024). 2023. URL: https://www. bdew.de/energie/studie-wie-heizt-deutschland/.
8. Hans-Martin Henning and Andreas Palzer. "A comprehensive model for the German electricity and heat sector in a future energy system with a dominant contribution from renewable energy technologies—Part I: Methodology". In: Renewable and Sustainable Energy Reviews 30 (2014), pp. 1003–1018.
9. Andreas Palzer and Hans-Martin Henning. "A comprehensive model for the German electricity and heat sector in a future energy system with a dominant contribution from renewable energy technologies–Part II: Results". In: Renewable and Sustainable Energy Reviews 30 (2014), pp. 1019–1034.
10. Bongghi Hong and Robert W Howarth. "Greenhouse gas emissions from domestic hot water: heat pumps compared to most commonly used systems". In: Energy Science & Engineering 4.2 (2016), pp. 123–133.
11. Hatef Madani and Erica Roccatello. "A comprehensive study on the important faults in heat pump system during the warranty period". In: International journal of refrigeration 48 (2014), pp. 19–25.
12. Qian Ning et al. "Flammable refrigerant leakage hazards control for splittype household air conditioners". In: International Journal of Refrigeration 144 (2022), pp. 188–201.
13. Shinichi Ito et al. "Influence of Low Concentration of Phosphorus on the Progression of Ant's Nest Corrosion". In: Zairyo-to-Kankyo 67 (Jan. 2018), pp. 37–40. DOI: 10.3323/jcorr.67.37.
14. D. Gary Harlow and Robert P. Wei. "Probability approach for prediction of corrosion and corrosion fatigue life". In: AIAA Journal 32.10 (1994), pp. 2073– 2079. DOI: 10.2514/3.12254. eprint: https://doi.org/10.2514/3.12254. URL: https://doi.org/10.2514/3.12254.
15. Luis A Escobar and William Q Meeker. "A review of accelerated test models". In: Statistical science (2006), pp. 552–577.
16. Danny Günther et al. "WP Monitor", Feldmessung von Wärmepumpenanlagen. Accessed: (26.02.2025). 2014. URL: https://wp- monitoring.ise. fraunhofer.de/wp-monitor-plus/download/endbericht_wp_monitor. pdf.
17. Ilaria Grossi et al. "Dynamic modelling and energy performance analysis of an innovative dual-source heat pump system". In: Applied Thermal Engineering 142 (2018), pp. 745–759.
18. statista. Monatliche Durchschnittstemperatur in Deutschland von Januar 2024 bis Januar 2025. https://de.statista.com/statistik/daten/studie/ 5564/umfrage/monatliche-durchschnittstemperatur-in-deutschland/. Accessed: (04.02.2025). 2025
19. Laenderdaten.info. Das Klima in Deutschland. https://www.laenderdaten. info/Europa/Deutschland/Klima.php. Accessed: (05.02.2025). 2025
20. V Brusic et al. "Copper corrosion with and without inhibitors". In: Journal of the electrochemical society 138.8 (1991), p. 2253.
21. alpha innotec. Lebensdauer einer Wärmepumpe. Accessed: (01.12.2025). URL: https://www.alpha-innotec.com/de/ratgeber/wissensquelle-warmepumpe/lebensdauer-einer-warmepumpe
22. Lovvorn, N C and Hiller, C C. "A study of heat pump service life." *ASHRAE Trans.; (United States)*, *vol. 91:2B*, Dec. 1984.